Supplemental Figure I

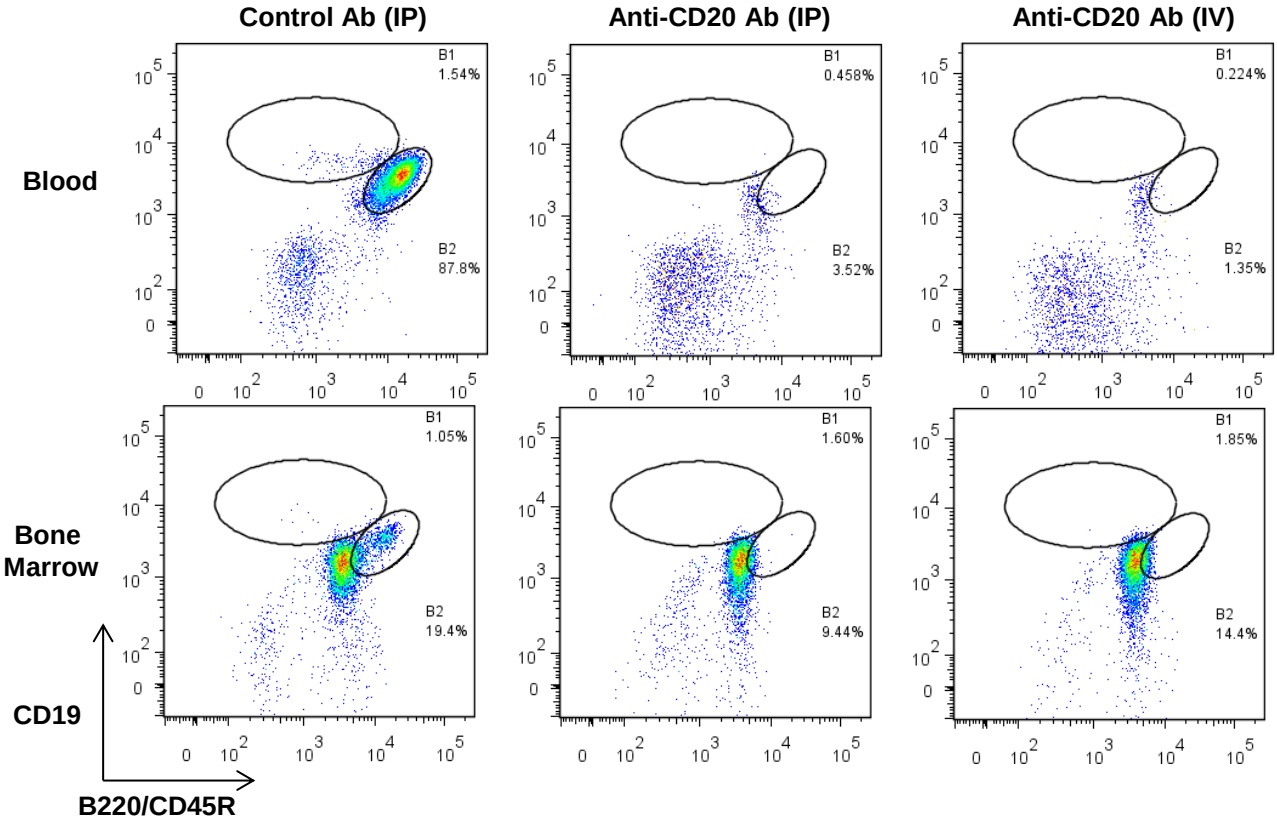

Supplemental Figure I: Anti-CD20 antibody-mediated depletion of B cells in mice. Representative flow cytometry plots showing depletion of B1 and B2 cells in blood and bone marrow of WT mice administered two doses of anti-CD20 antibody either *via* IP or IV. WT mice were also injected with control antibody *via* IP as negative control.

Supplemental Figure II

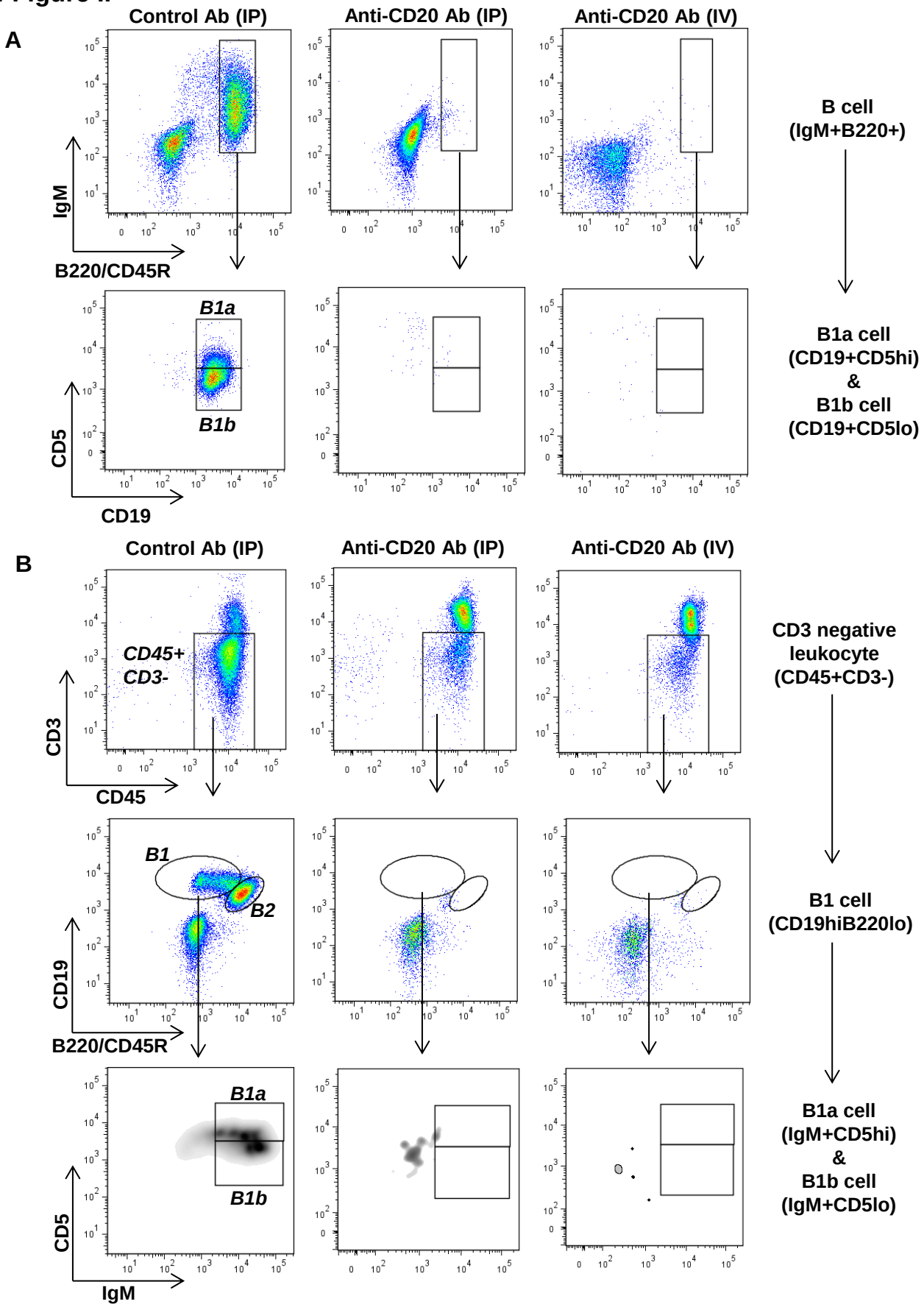

Supplemental Figure II: Anti-CD20 antibody-mediated depletion of B cells in peritoneal cavity. Representative flow cytometry plots showing depletion of B1a and B1b cells *via* two methods of characterization (**A** and **B**) in peritoneal fluid of WT mice administered two doses of anti-CD20 antibody either *via* IP or IV. WT mice were also injected with control antibody *via* IP as negative control. A schematic presentation of the gating is also shown.

Supplemental Figure III

A **Study design for B cell depletion and induction of AngII-induced aortic aneurysm**

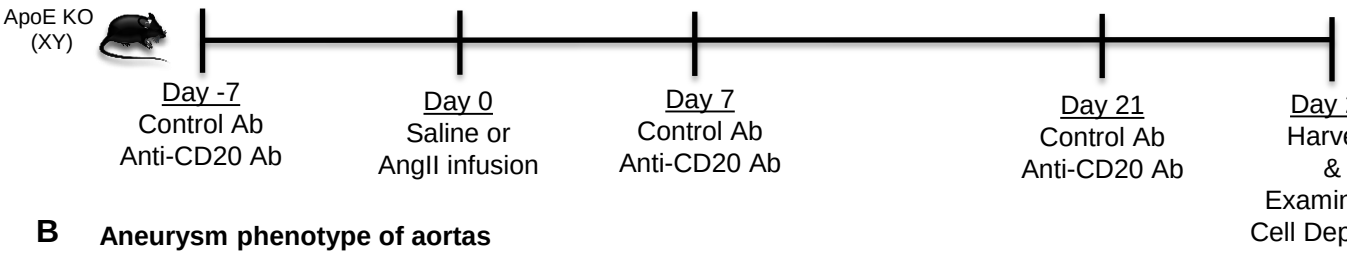

B **Aneurysm phenotype of aortas**

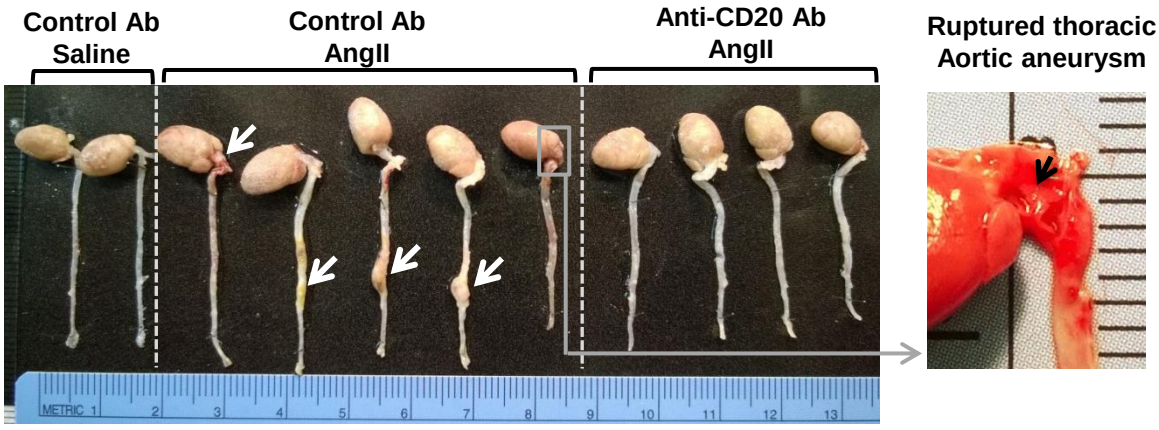

C **AAA stage (%)**

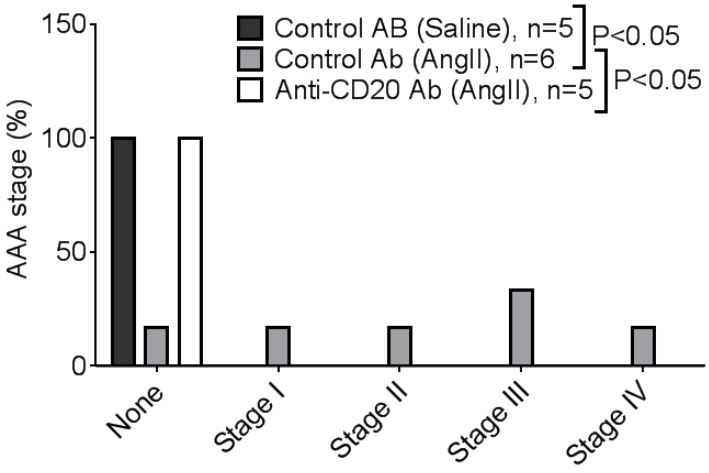

D **Plasma aldosterone (pg/ml)**

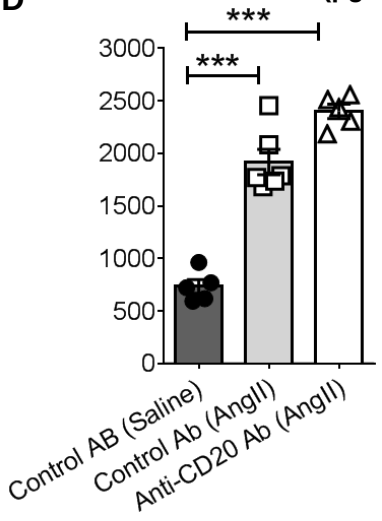

E **VVG staining of suprarenal aorta showing elastin degradation**

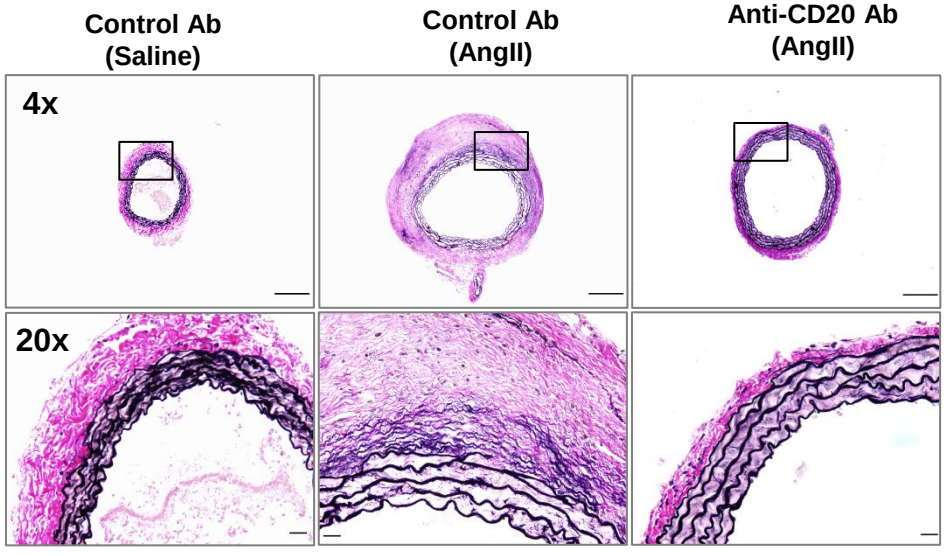

Elastic fiber area (%)

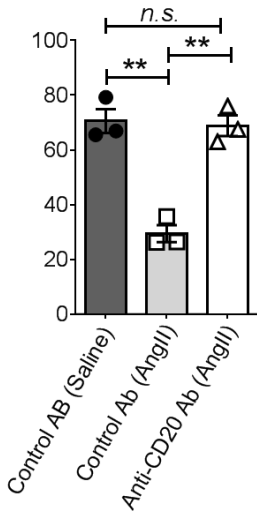

Adventitial area (μm²)

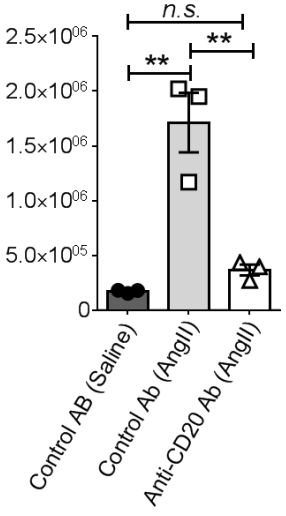

Continued

Supplemental Figure III: Figure 3: B cell depletion suppresses AngII infusion-induced aortic aneurysm in ApoE KO mice. A, Schematic representation of study design for B cell depletion and induction of experimental AngII infusion model of murine AAA. **B**, Photograph showing aneurysm pathology. Arrows indicate the site of aneurysm. An enlarged image of ruptured thoracic aneurysm is shown in the right panel. **C**, Quantification of stages of aneurysm: Control antibody treated and infused with saline, n= 5; Control antibody treated and infused with AngII, n=6 and Anti-CD20 antibody treated and infused with AngII, n=5. To determine the significant difference in aneurysm pathology between two groups, multiple t-test was used, in which, aneurysm pathology score of each mouse was entered into side-by-side subcolumns all in a row for a group and unpaired t test with fewer assumptions was applied. **D**, Quantification of plasma aldosterone as a measure of AngII infusion (n=5-6). Following one-way ANOVA, parametric unpaired t-test was applied to determine significant differences between the groups. **E**, Representative images showing AAA sections stained for Verhoeff-Van Gieson or VVG (elastic fibers, black). A small segment of images acquired in 4x is shown in 20x magnification. Scale bar in 4x images is 500 µm and in 20x images is 50 µm. Elastic fiber area (presented as percentage of total aortic area) and adventitial area were determined using ImageJ. Following one-way ANOVA, non-parametric t-test (Mann-Whitney test) was applied to determine significant differences between the groups. Values are expressed as means ± SEM, "**" and "***" indicate $p < 0.01$ and 0.001, respectively.

Supplemental Figure IV

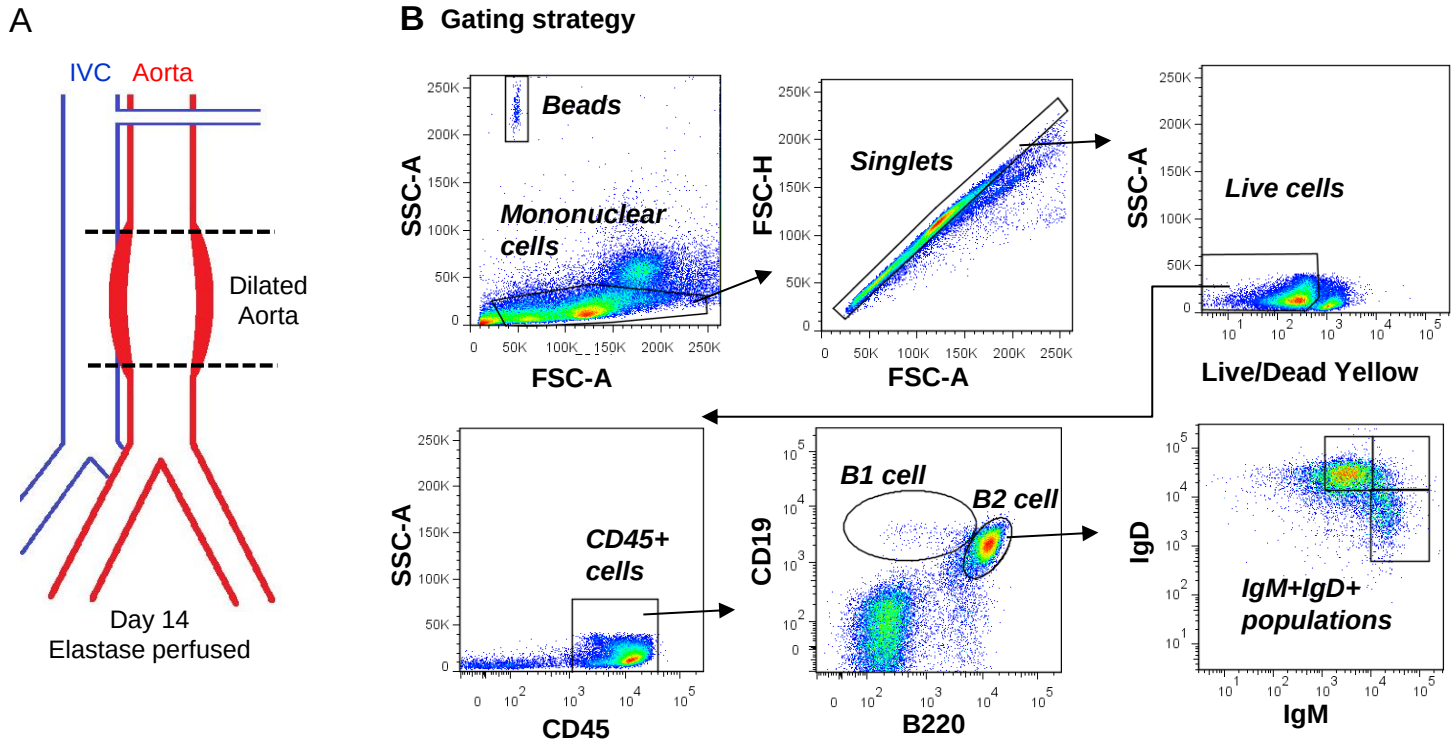

Supplemental Figure IV: Schematic presentation of aorta harvested and gating strategy of flow cytometry method. A, Schematic presentation showing specific segment of the aorta (region within the dotted line) was harvested for flow cytometry, gene expressing analysis and immunohistochemistry. **B**, Representative flow cytometry plots from mouse splenocytes showing gating strategy used in the current study. Based on scattering properties, mononuclear cells were gated, followed by gating singlets and live cells. The live cells were further gated for CD45+, followed by B1 and B2 cells and IgM+IgD+ populations.

Supplemental Figure V

WT mice

Aorta

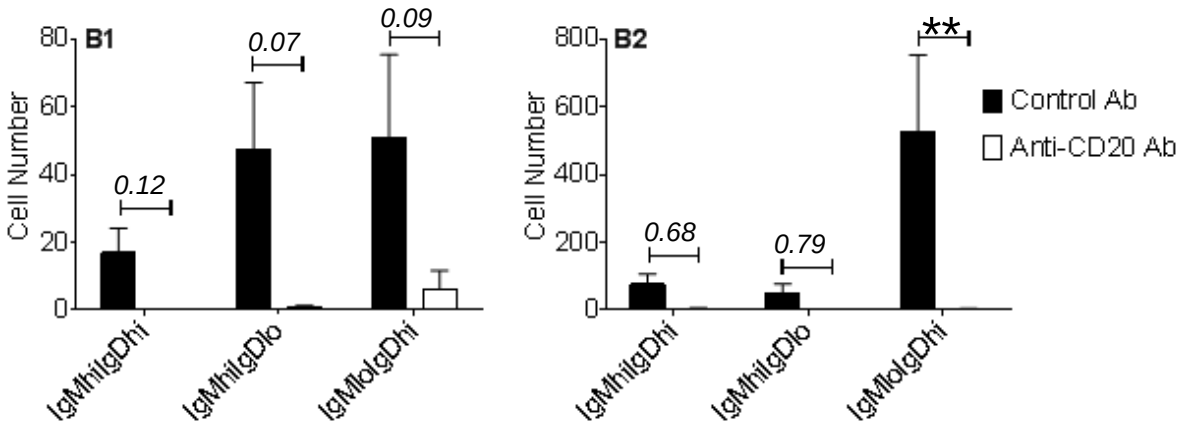

Spleen

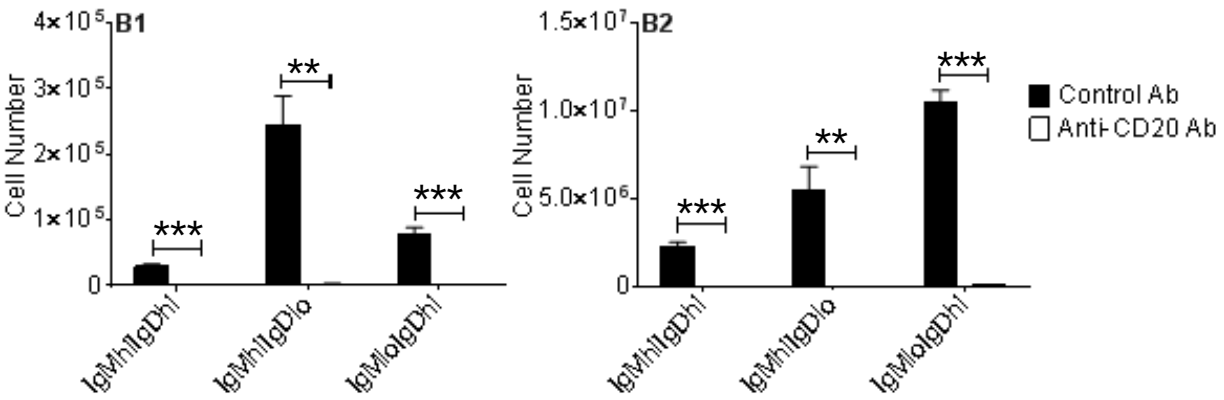

Supplemental Figure V: IgM and IgD populations in aorta and spleen. Quantification of IgM+IgD+ populations in B1 and B2 cells from AAA and spleen of WT mice administered two doses of control or anti-CD20 antibody *via* IV. Following one-way ANOVA, non-parametric t-test (Mann-Whitney test) was applied to determine significant differences between the groups. Values are expressed as means ± SEM (n=3-5) and "*", "**" and "***" indicate $p<0.05$, 0.01 and 0.001, respectively. 'p' values >0.05 are indicated.

Supplemental Figure VI

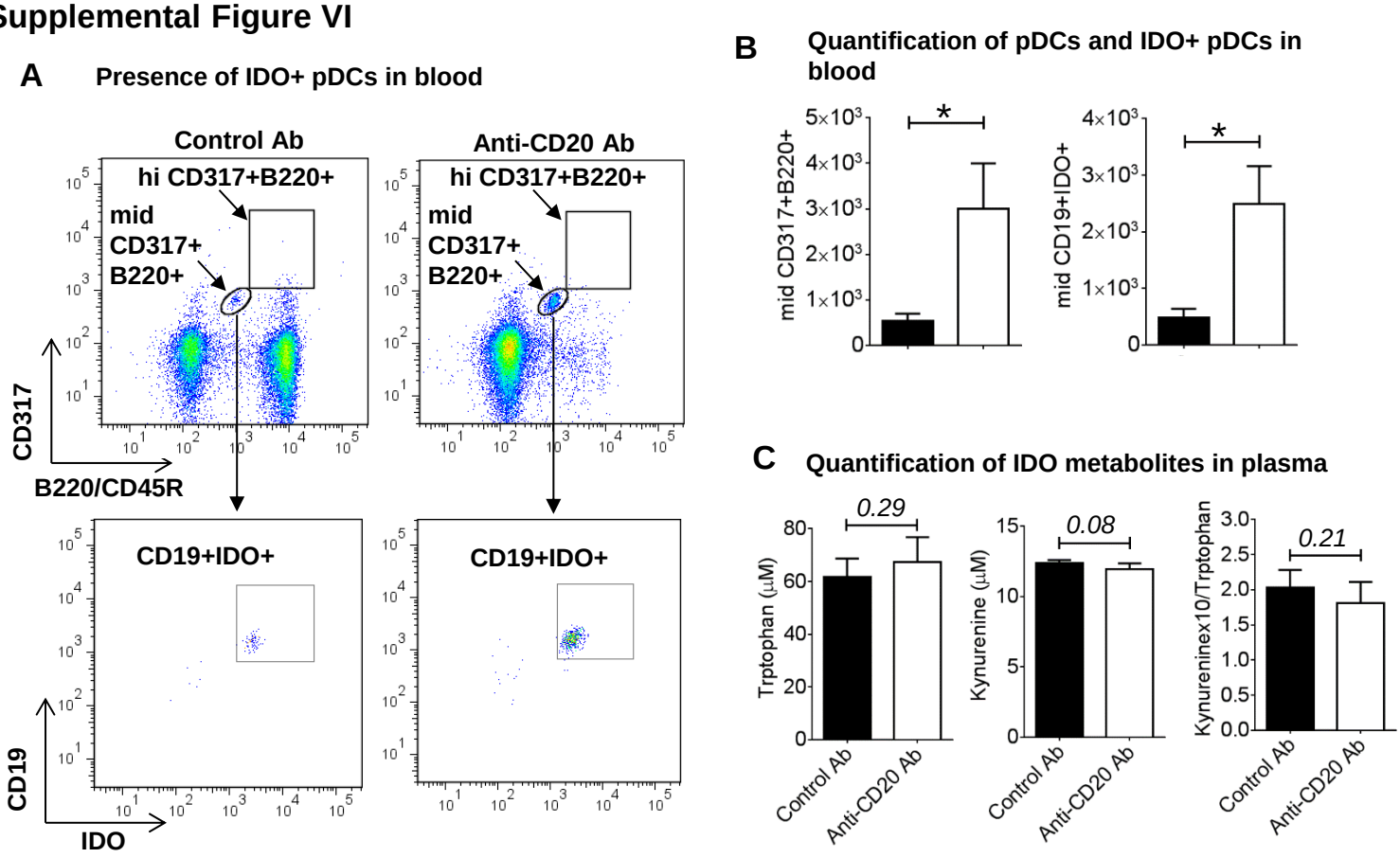

Supplemental Figure VI: The number of IDO expressing pDC is increased in the blood of B cell depleted mice. **A**, Representative Flow cytometry plots showing gating and increase in concentration of mid B220+CD317+CD19+IDO+ cells in blood (100 µl) following anti-CD20 antibody treatment *via* IV. The cells have been gated for singlets, live, CD45+ and CD4- mononuclear cells. **B**, Increase in number of mid CD317+B220+ and mid CD19+IDO+ cells following anti-CD20 antibody treatment (n=3-4). **C**, Quantification of Tryptophan and Kynurenine, and Kynurenine-Tryptophan ratio following anti-CD20 antibody treatment (n=4-5). Non-parametric t-test (Mann-Whitney test) was applied to determine significant differences between the groups. "*" indicates $p<0.05$. 'p' values >0.05 are indicated.

Graphic Abstract